Nanoscale

Accepted Manuscript

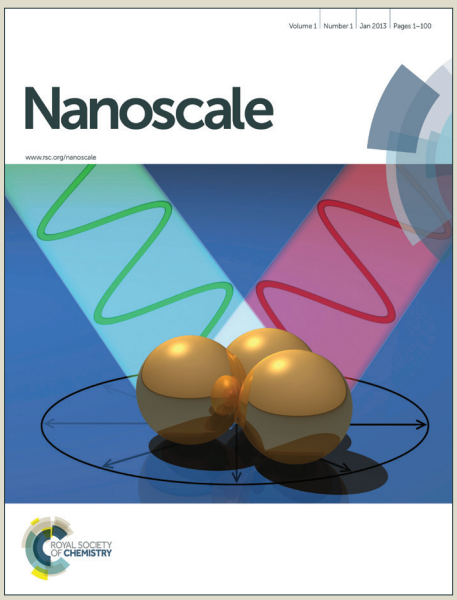

ROYAL SOCIETY OF CHEMISTRY

www.rsc.org/nanoscale

Cite this: DOI: 10.1039/c0xx00000x

www.rsc.org/xxxxxx

ARTICLE TYPE

Porous Pd Nanoparticles with High Photothermal Conversion Efficiency for Efficient Ablation of Cancer Cell

Jia-Wen Xiao, Shi-Xuan Fan, Feng Wang, Ling-Dong Sun,* Xiao-Yu Zheng and Chun-Hua Yan*

Received (in XXX, XXX) Xth XXXXXXXXX 20XX, Accepted Xth XXXXXXXXX 20XX

DOI: 10.1039/b000000x

Nanoparticle (NP) mediated photothermal effect shows great potential as a noninvasive method for cancer therapy treatment, but the development of photothermal agent with high photothermal conversion efficiency, small size and good biocompatibility is still a big challenge. Herein, we report the Pd NPs with special porous structure exhibit enhanced near infrared (NIR) absorption compared with Pd nanocubes with similar size (almost two-fold enhancement with a molar extinction coefficient of $6.3\times10^7\ M^{-1}\cdot cm^{-1}$), and the porous Pd NPs display monotonically rising absorbance from NIR to UV-Vis region. When dispersed in water and illuminated with an 808 nm laser, the porous Pd NPs give a photothermal conversion efficiency as high as 93.4%, which is comparable to the efficiency of Au nanorods we synthesized (98.6%). As the porous Pd NPs show broadband NIR absorption (650-1200 nm), it allows us to choose multiple laser wavelengths for photothermal therapy. *In vitro* photothermal heating of HeLa cells in the presence of porous Pd NPs leads to 100% cell death under 808 nm laser irradiation (8 W/cm^2, 4 min). For photothermal heating using 730 nm laser, 70% of HeLa cells were killed after 4 min irradiation at a relative low power density of 6 W/cm^2. These results demonstrated that the porous Pd nanostructure is an attractive photothermal agent for cancer therapy.

Introduction

Nanoparticle (NP) mediated photothermal therapy (PTT) has attracted extensive interests in recent years by virtue of its noninvasive feature and minimal side effects compared with traditional methods, such as surgery and chemotherapy.[1] In this PTT protocol, NPs absorb photon energy and convert it into heat locally, resulting in a local temperature rise which causes the death of cancer cells and tissues. As for the light source, near-infrared (NIR) light (650–950 nm) is generally favored, as it can penetrate tissues deeply because of the relatively low absorption by hemoglobin and water in tissues and less damage to biological tissues.[2,3] Therefore, NPs used in PTT are expected to have strong absorption in the NIR region, high photothermal conversion efficiency, as well as good biocompatibility. Also, considering size effect, the NPs as PTT agent are preferred to have relatively small sizes (typically ranging around 10–50 nm),[4] so as to increase their bloodstream circulation time and to enhance the cellular uptake probability.[5-7]

In the past few years, different types of photothermal agents have been developed for cancer therapy *in vitro* and *in vivo*, including organic nanomaterials (*e.g.*, indocyanine green[8] and polypyrrole[9]), carbon nanomaterials (carbon nanotube[10] and nanographene[11,12]), metal nanostructure (Au nanomaterials[1] and Pd nanosheet[13]) and copper sulfide or selenide NPs[14-16]. Among these materials, Au nanostructures (such as nanorods,[17-19] nanoshells[20] and nanocages,[21] gold nanostars[22] or nanohexapods[23]) are the most-widely studied for PTT application because of their high optical extinction coefficients in the NIR region resulting from surface plasmon resonance (SPR) absorption. However, the Au nanostructures for PTT are generally large in size. For instance, the Au nanorods used are typically ~10 nm in width, ~ 50 nm in lengths,[18,24] and Au nanoshells, which are typically above 100 nm.[25,26] Furthermore, the anisotropic or hollow Au nanostructures lack of good thermal stability. They have the tendency to transform into nanospheres when exposed to NIR laser, accompanied with the disappearance of the NIR absorption band.[27,28] Recently, metal NPs other than Au have also been explored. Notably, ultrathin Pd nanosheets synthesized by Huang were demonstrated to generate heat under NIR laser to kill cancer cells;[13] however, the 2-dimensional ultrathin nature prevents Pd sheets from efficiently entering cancer cells.[29] It is still of great necessity to develop strong NIR-absorbption NPs with suitable size and good thermal stability.

Besides SPR absorption, metal NPs also possess interband transition absorption. Notably, Pd NPs show very broad absorption through the UV-vis-NIR region. This broad absorption nature would help to extend our choices on the wavelengths of NIR lasers in PTT application. Also, properly controlling the architecture of NPs may allow us to obtain strong NIR-absorbing Pd NPs.[13] Here in this work, we report the preparation of small and monodisperse Pd NPs with a special porous structure and enhanced NIR absorption compared with solid Pd NPs. These porous Pd NPs show a high photothermal conversion efficiency (93.4%), which is comparable with the most studied Au nanorods (98.6% with our measurement method). And using the porous Pd NPs, the effective photothermal killing of cancer cells with relatively low power density, at two different NIR wavelengths

(730 nm and 808 nm) were demonstrated.

Experimental

Chemicals and reagents

$PdCl_2$ was purchased from Shenyang Nonferrous Metal Research Institute, Poly(ethylene glycol) monomethylether thiol (mPEG-SH, Mw ≈ 5000), cetyltrimethylammonium bromide (CTAB), cetyltrimethylammonium chloride (CTAC), and $NaBH_4$ were purchased from Sigma-Aldrich. Ascorbic acid, hydrochloric acid, and concentrated nitric acid were obtained from Xilong chemical industry company (Guangdong Province).

Synthesis of porous Pd NPs

The synthesis of porous Pd NPs was carried out by adapting a procedure reported by Wang et al.[30] Aqueous H_2PdCl_4 solutions (0.01 M) were prepared by completely dissolving 44.5 mg (0.25 mmol) $PdCl_2$ in HCl (0.02 M, 25 mL) at 50 ºC. In a typical synthesis procedure, H_2PdCl_4 (0.01 M, 0.25 mL) and CTAC (0.1 M, 9.75 mL) was first mixed together. A freshly prepared, ice-cold $NaBH_4$ solution (0.01 M, 0.60 mL) was added to the mixed solution under vigorous stirring. The resultant solution was kept undisturbed for 2 h at room temperature as seed solution. For the growth of the Pd nanoparticles, the seed solution (0.025 mL) was added to a mixture solution made of CTAC (4.5 mM, 9.70 mL) and H_2PdCl_4 (0.01 M, 0.30 mL), followed by the addition of ascorbic acid (0.1 M, 0.1 mL). The reaction solution was mixed by gentle inversion for 10 s and then left undisturbed at room temperature for 6 h.

Synthesis of Pd nanocubes

The Pd nanocubes were synthesized according to a reported procedure.[31] Briefly, the H_2PdCl_4 solution (0.01 M, 0.5 mL) was added into an aqueous CTAB solution (0.0125 M , 10 mL). The mixture solution was then heated to 96 ºC and kept at this temperature for 20 min, followed by the addition of an aqueous AA solution (0.1 M, 0.08 mL). The resultant solution was kept at the same temperature for another 30 min for the growth of nanocubes. The as-prepared Pd nanocube solution was centrifuged at 18000 rpm for 15 min. The precipitate was then dispersed in water (2 mL) for further use.

Synthesis of small sized Pd NPs and polyhedron

The small sized Pd NPs were synthesized by directly reduction of H_2PdCl_4 (0.01M, 0.25 mL) by freshly prepared ice-cold $NaBH_4$ solution (0.01 M, 0.60 mL) in the presence of CTAC as surfactant. The broad sized Pd polyhedron was synthesized by solvothermal method. Typically, Na_2PdCl_4 (0.030 mmol, obtained by dissolving 1.0 g of $PdCl_2$ and 0.66 g of NaCl with 100 mL of water at room temperature under stirring overnight), and PVP (100 mg) were dissolved in 10 mL of water. The pH value of the solution was adjusted to about 3 by adding drops of HCl (1.0 M) solutions and the total volume of the solution was kept at 15 mL. The homogeneous dark red solution was transferred to a 25 mL Teflon-lined stainless steel autoclave and sealed. The autoclave was then heated at 160 °C for 4 hours. The black nanoparticles were centrifuged by adding 45 millilitres of acetone and further washed by acetone/water for several times.

Photothermal effect measurement of Pd NPs

To study the photothermal effect induced by the strong NIR absorption, 2 mL aqueous solutions containing different concentration (0, 15, 25 and 50 ppm) of porous Pd NPs were irradiated by a NIR laser (808nm, 1.6 W) for 10 min. The temperatures of the solutions were monitored by a thermocouple microprobe submerged in the solution in a 1-cm square cuvette. The probe was placed at such a position that the direct irradiation of the laser on the probe was avoided. For comparing the photothermal conversion efficiency of porous Pd NPs with that of Au nanorods, the optical density at 808 nm of porous Pd NPs and Au nanorods were adjusted to 1.0. Then their photothermal effect was measured as described above, and the cooling curve was obtained after the laser was switched off.

Surface modification of porous Pd NPs with HS-PEG

To decrease the cytotoxicity of porous Pd NPs, the surfactant CTAC should be removed as much as possible. The ligand exchange method is used to remove the surface capped CTAC molecules. In a typical procedure, 10 mL of porous Pd NPs dispersion (about 100 μg/mL) was mixed with 500 μL of HS-PEG (500 mg/mL) aqueous solution. The mixed solution was stirred overnight. And then the HS-PEG capped Pd NPs were collected by centrifugation at 18000 rpm for 15 min. This ligand exchange procedure was repeated for 3 times to wipe off the CTAC molecules sufficiently. After the ligand exchange process, the porous Pd NPs were re-dispersed in 1 mL ultrapure water for further use.

In vitro cytotoxicity evaluation of porous Pd NPs

HeLa Cells were pre-cultured in a 96-well plate for 24 h, and then porous Pd NP dispersions with a series of concentrations were added to the culture media. After continuous incubation for 24 h, the cells was washed with fresh culture media twice. Then a cell viability assay agent, CCK-8, was added to the media. After incubation for 30 min, the 96-well plate was taken out and the absorbance of each well was collected to calculate the number of viable cell.

Evaluating the photothermal performance of porous Pd NPs *in vitro*

HeLa cells were cultured at 37 °C and 5 % CO_2 in Dulbecco's Modified Eagle Medium (DMEM) supplemented with 10 % fetal bovine serum (FBS), 1 % penicillin/streptomycin.

For photothermal therapy study, HeLa cell suspension (100 μL, 1×10^4 cells per well) was dispensed into a 96-well plate and pre-incubated at 37 °C and 5 % CO_2 for 24 h. Then the as-prepared nanomaterial colloid solution (250 μg/mL, 10 μL) was added into each well of the plate (n=4). The 96-well plate was incubated for another 6 h in the incubator. Subsequently, HeLa cells treated or not treated with Pd NPs were exposed to a 808 nm laser with 8 W/cm^2 for 4 min. After laser irradiation, the Hela cells were washed with fresh culture media twice to remove the excess Pd NPs. After that, the Hela cells were incubated for another 4 h. Next the standard CCK-8 assay was conducted to obtain the cell viability. Photothermal ablation of cancer cells using 730 nm laser was done in the same way. After laser irradiation, the cells were also stained by Calcein acetoxymethyl ester (Calcein AM)

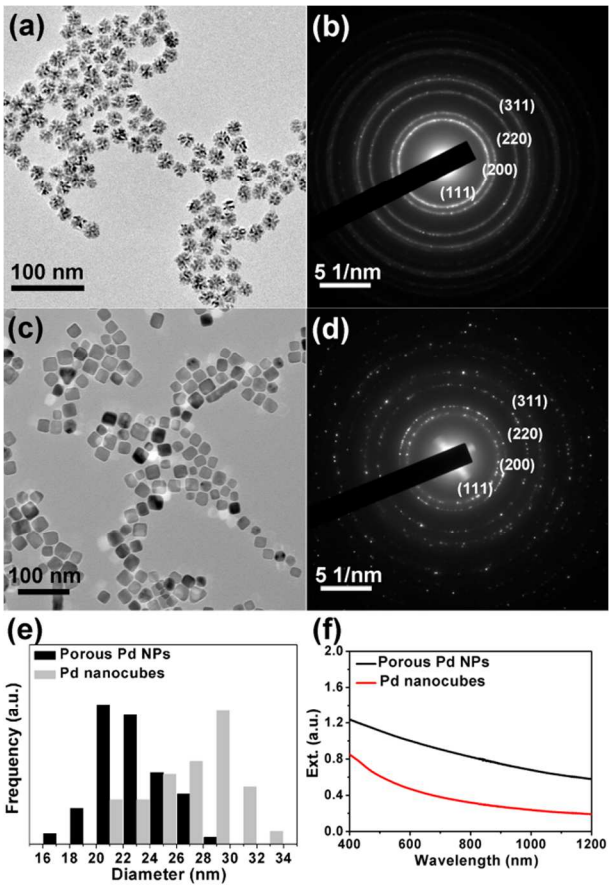

Figure 1 (a, b), (c, d) TEM images and the corresponding SAED pattern of the as-synthesized porous Pd NPs and Pd nanocubes, respectively. (e) Size distribution of porous Pd NPs and Pd nanocubes obtained by calculating more than 100 NPs. (f) The typical extinction spectra of porous Pd NPs and Pd nanocubes dispersed in water with same mass concentration (50 μg/mL).

and propidium iodide (PI) to directly observe the live and dead cells under fluorescence microscope. For details, the cells were washed with phosphate buffer solution (PBS) twice after laser illumination, and then a PBS solution containing Calcein AM and PI was added to the wells to stain HeLa cells for 10 min under dark place. After dye staining the HeLa cells were washed with PBS twice again and fresh PBS solution was added. Fluorescence images of live and dead HeLa cells were obtained by fluorescence microscope.

Instrument and characterization

The UV-Vis-NIR extinction spectra were acquired using a Shimadazu UV3100 Spectrometer. The TEM images of Pd NPs and Au nanorods were obtained using JEOL JEM 2100 transmission electron microscope operated at 200 kV. The mass concentration of Pd NPs and Au nanorods was determined by inductively coupled plasma atomic emission spectroscopy (ICP-AES). The NPs were decomposed in concentrated HNO_3 around 100 ºC.

Results and discussion

The porous Pd NPs were synthesized by a seed mediated growth method according to a reported procedure (see experimental for details).[30] The typical TEM image of the as-synthesized porous Pd NPs is shown in Figure 1a. The porous Pd NPs with uniform size is single crystalline, which has been verified in the previous work[30]. Figure 1b demonstrated the selected area electron diffraction (SAED) pattern of porous Pd NPs. The distinct diffraction ring can be well indexed to the cubic phase of Pd crystals. The average size of porous Pd NPs is 22.8 ± 2.5 nm (Figure 1e). In order to compare the absorption property of our porous Pd NPs with solid Pd nanocrystals, Pd nanocubes were chosen because of its simple preparation procedure. As shown in Figure 1c, the as-prepared Pd nanocubes are 26.9 ± 3.2 nm in edge, slightly larger than that of our porous Pd NPs. And the SAED pattern of Pd nanocubes confirms the cubic phase of Pd crystals (Figure 1d).

Interestingly, we found that the porous Pd NPs exhibit higher absorption than solid Pd nanocubes at the same mass concentration (μg/mL). As illustrated in Figure 1f, both the porous Pd NPs and Pd nanocubes in water show monotonically rising absorbance from NIR to UV-vis region. Although the surface plasmon resonance of Pd NPs is not located in the vis-NIR region,[31] the porous Pd NPs display notable absorbance in NIR region, which qualifies these porous Pd NPs as a potential photothermal agent. It is worth noting that the absorbance of porous Pd NPs is nearly two times of Pd nanocubes at the same mass concentration, which is the most significant result of this study. We speculate that this enhanced absorption may come from the free electron oscillation coupling of the small domain of single porous Pd NP. To further illustrate the absorbance enhancement effect of porous Pd NPs, we compare the extinction spectra of porous Pd NPs with small sized Pd NPs and similar sized Pd polyhedral (Figure S1 in Supporting Information). From Figure S1 we can see that the NIR absorbance of porous Pd NPs is higher than both of the small sized Pd NPs and Pd polyhedral. The absorbance of porous Pd NPs is almost three times of small sized Pd NPs. This data support that the absorbance of porous Pd NPs is not a simple sum of small domain of porous Pd NPs. Instead, the interaction among small domain of porous Pd NPs should be taken into account. Furthermore, as the porous Pd NPs show broad and strong absorption through the entire NIR regions, multiple NIR laser wavelengths could be chosen for PTT. Since the size of porous Pd NPs is relatively small (about 20 nm), the majority of optical extinction comes from light absorption rather than light scattering. So the porous Pd NPs are expected to exhibit high photothermal conversion efficiency.

To quantitatively compare the absorption property of porous Pd NPs with other photothermal agents, the molar extinction coefficient was calculated by the measured absorbance with equation (1) [32] below

$$\varepsilon = (AV_{NP}\rho N_A)/(LC) \quad (1)$$

where ε is the molar extinction coefficient of porous Pd NPs, A is the optical density of porous Pd NPs dispersion with a mass concentration of C, V_{NP} is the average volume of single porous Pd NP, ρ is the density of Pd NPs assuming that it is the same with that of the bulk Pd metal, N_A is the Avogadro's constant (6.02×10^{23} mol^{-1}), and L is the light path length (1 cm in the current case).

Assuming a spherical-like shape, the volume of a NP could be

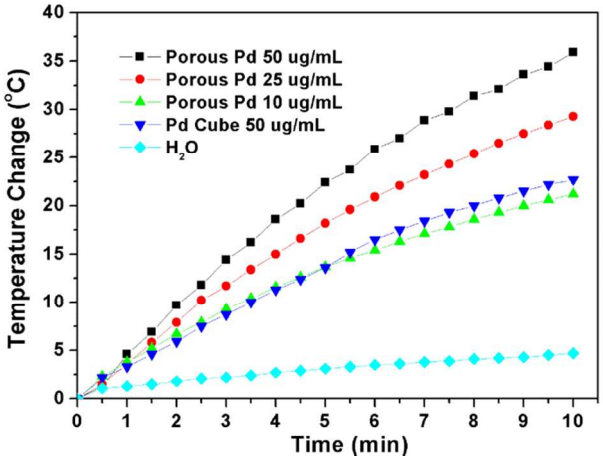

Figure 2 Photothermal heating curves of porous Pd NPs and Pd nanocubes in water with various concentrations. 2 mL Pd NP colloidal solution was illuminated by an 808 nm laser (8 W/cm^2) for 10 min, and the temperature increase from porous Pd NPs is significantly higher than that of Pd nanocubes.

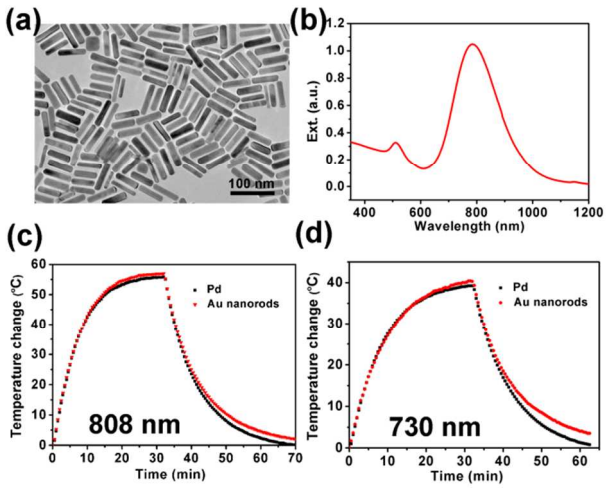

Figure 3 TEM image (a) and extinction spectra (b) of the as-synthesized Au nanorods. The average size of Au nanorods is 60.8 ± 5.5 nm in length, 14.6 ± 2.0 nm in width. (c, d) Temperature plots of heating and cooling process for porous Pd NPs and Au nanorods dispersion illuminated by 808 nm laser (8 W/cm^2) and 730 nm laser (6 W/cm^2).

calculated with the size from the TEM images, the calculated molar extinction coefficient at 808 nm is 6.3×10^7 $M^{-1}\cdot cm^{-1}$. This value is higher than that of carbon nanotube (r=0.6 nm, L=150 nm, ~7.9×10^6 $M^{-1}\cdot cm^{-1}$ at 808 nm),[33] similar to that of $Cu_{2-x}Se$ NPs (7.7×10^7 $M^{-1}\cdot cm^{-1}$ at 980 nm),[16] but lower than that of gold nanorods (r=5 nm, L=27 nm, 1.9×10^9 $M^{-1}\cdot cm^{-1}$)[34] or nanoshells (r_1=55 nm, r_2=65 nm, ~2×10^{11} $M^{-1}\cdot cm^{-1}$ at 800 nm).[25]

Next we compared the photothermal effect of our porous Pd NPs with Pd nanocubes. The photothermal effect was measured by irradiating 2 mL of aqueous NPs dispersion with an 808 nm laser (output power 1.6 W) for 10 min. For both porous Pd NPs and Pd nanocubes, the mass concentration was adjusted to 50 μg/mL. The results were summarized in Figure 2, from which we can find that the temperature rising for porous Pd NP dispersion is obviously faster than that of solid Pd nanocube dispersion. After 10 min irradiation, the temperature of the former was increased by 36 ºC, while the latter, by 22.7 ºC. We also conducted experiments with lower concentrations of porous Pd NPs. It was found that, at a concentration as low as 10 μg/mL, the porous Pd NPs showed a similar heating effect to solid Pd nanocubes at 50 μg/mL. These data confirmed that the porous Pd NPs are superior to solid Pd nanocubes in photothermal effect.

The photothermal conversion efficiency of the porous Pd NPs was also measured, with Au nanorods as a reference. The optical density at 808 nm was adjusted to be 1.000 for porous Pd NPs and Au nanorods dispersion. The NP dispersions were irradiated by a NIR laser until reaching a steady-state temperature. The NIR laser was then switched off and the temperature decrease profile was recorded to determine the rate of heat transfer from the system. Figure 3a shows the TEM image of the Au nanorods we synthesized, with an average size of 60.8 ± 5.5 nm in length, 14.6 ± 2.0 nm in width. And the longitude plasmon resonance wavelength of Au nanorods is centered at 800 nm (Figure 3b). An 808 nm laser was used as the light source, with output power of 1.6 W, and the temperature was recorded as a function of irradiation time. As illustrated in Figure 3c, the profile for porous Pd NPs is quite similar to that for Au nanorods. According to these data and using the method developed by Wang,[35] the photothermal conversion efficiency η, was calculated using the following equation

$$\eta = \frac{B(T_{end}-T_0)+C(T_{end}-T_0)^2-I\xi}{I(1-\xi)(1-10^{-A})} \quad (2)$$

where I=1.3 W is the reflection-corrected laser output power, A is the extinction value at 808 nm, B and C ($J\cdot K^{-1}\cdot min^{-1}$) are two coefficients describing the heat transfer rate of the system, which are obtained by fitting the temperature decrease curve. T_0 is the temperature of the solution before laser irradiation; T_{end} is the steady temperature during the laser illumination. And ξ is the fraction of the laser energy absorbed by the cuvette walls and the solution. The value of ξ is determined by measuring the temperature rising and decay curves of pure water. In this case, the value of ξ was determined to be 0.135. By using equation (2) we obtained that the photothermal conversion efficiency is 93.4% for porous Pd NPs, slightly lower than that of Au nanorods (98.6%) (see Tables S1 and S2 in Supporting Information for detailed calculation). This result is reasonable because the molar extinction coefficient of porous Pd NPs is much lower than that of Au nanorods. We also measured the photothermal conversion efficiency of Pd NPs and Au nanorods using a 730 nm laser. In this case, the porous Pd NPs gave a photothermal conversion efficiency of 95.6%, much higher than that for Au nanorods (85.6%). As we know the extinction capability of metal NPs at LSPR peak wavelength would be tremendously enhanced, whereas the LSPR peak wavelength of Au nanorods we synthesized is far from 730 nm, so the extinction coefficient of Au nanorods at 730 nm is relatively low. Otherwise, as the size of Au nanorods is much larger than that of porous Pd NPs, the fraction of scattering in the extinction would be higher, which may also decrease the photothermal conversion efficiency of Au nanorods.

We further investigate the *in vitro* efficacy of the porous Pd NPs as photothermal agent. Since the as-prepared NPs were capped with CTAC surfactant (which is highly toxic for cells), we performed PEG-SH coating so as to improve the biocompatibility. Methoxy-terminated PEG-thiol (mPEG-SH,

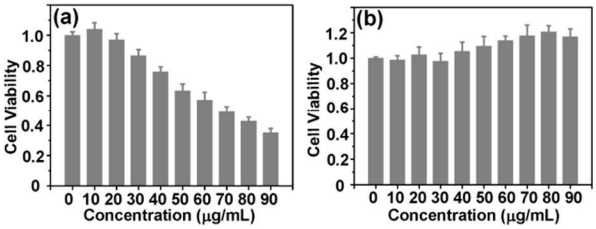

Figure 4 In vitro cytotoxicity evaluation based on CCK-8 assay for (a) HeLa cells incubated for 24 h with porous Pd NPs, (b) A549 cells incubated for 24 h with porous Pd NPs.

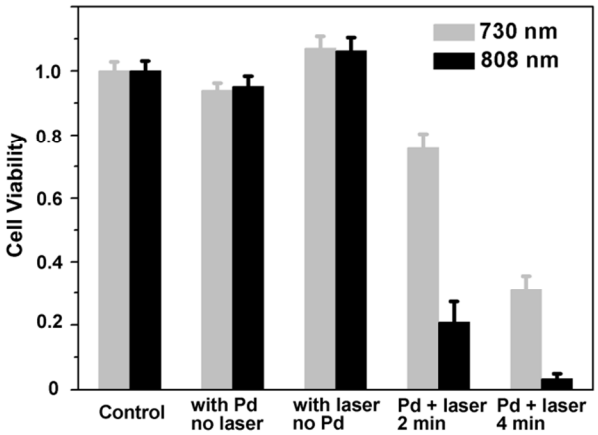

Figure 5 Cell viability of HeLa cell treated with or without porous Pd NPs after NIR laser irradiation. The porous Pd NPs dispersion was added to cell culture media to a concentration of 23 μg/mL. After incubation for 6 h, cells were irradiated with a 808 nm laser (8 W/cm^2) and a 730 nm laser (6 W/cm^2) for certain duration. Then the CCK-8 assay was conducted to measure the cell viability.

Mw=5,000) was added to the colloidal solution to replace the CTAC, and the modified NPs were purified by centrifugation. The zeta potential of porous Pd NPs measured by dynamic light scattering (DLS) is 35.2 mV before modification, in contrast to -2.4 mV after mPEG-SH coating, which suggests that most of the CTAC molecules capped on particle surface had been removed. The modified NPs also showed good dispersity in water, as revealed in the TEM images in Figure S2 in Supporting Information.

The cytotoxicity of porous Pd NPs was studied by conducting a cell viability assay of several cell lines. As shown in Figure 4, the half maximal inhibitory concentration (IC50) of porous Pd NPs is about 70 μg/mL for HeLa cells. Note that the concentration of Pd NPs we used for in vitro photothermal therapy is ~23.0 μg/mL, which is well below IC50 threshold. We found that the modified porous Pd NPs show good biocompatibility for the A549 cells (human lung carcinoma cell line). The cell viability still remains 100% when the concentration of porous Pd NPs is as high as 90 μg/mL.

To evaluate the efficacy of PTT of the porous Pd NPs, HeLa cells were incubated with porous Pd NPs at a concentration of 23 μg/mL. After incubation for 6 h at 37 ºC, the cells were illuminated with an 808 nm laser for certain duration. The results in Figure 5 show that 80% of HeLa cells were dead after 808 nm laser irradiation at a power density of 8 W/cm^2 for 2 min, and the cell viability decreased to near zero after 4 min irradiation. In contrast, cells without porous Pd NPs treatment or without laser illumination were still alive with no change in cell viability. As discussed before, since the porous Pd NPs exhibit broad absorption in the NIR region, multiple laser wavelengths can be chosen for photothermal cell ablation. We also used a 730 nm laser with a power density of 6 W/cm^2 to irradiate the cells. Figure 5 show that almost 25% of the HeLa cells treated with porous Pd NPs were killed after irradiated for 2 min and 70% of HeLa cells were ablated when irradiated for 4 min, while all the control groups show nearly 100% cell viability. The laser power density and the concentration of porous Pd NPs are vital parameter in photothermal ablation of cancer cells. We conducted the cell experiment at different laser power density and different mass concentration of porous Pd NPs by using Calcein AM and PI for live-dead assay (see experimental section), the results were presented in Figure S3 in Supporting Information. Under the power density of 6 W/cm^2 of 808 nm laser, no significant cell death was observed even after 10 min irradiation (concentration of Pd NPs 24 μg/mL). When the power density increased to 9 W/cm^2, obvious decreased cell viability emerged at the mass concentration of 18 μg/mL of porous Pd NPs after illumination for 5 min. The power density we used here for non-targeted PTT is much lower than that of $Cu_{2-x}Se$ NPs (30 W/cm^2)[16] and hollow Au nanoshell (40 W/cm^2)[36], which means that the porous Pd NPs we produced is an efficient photothermal therapy agent.

Furthermore, we compared the photothermal stability of porous Pd NPs with Au nanorods. As illustrated in Figure S4, we could clearly observed that some gold nanorods after laser irradiation (30 W/cm^2 for 30 min) melt into irregular shaped Au NPs and the extinction spectrum of Au nanorods broadened and blue shift, while no obvious variation was observed about the shape and extinction property of porous Pd NPs before and after laser irradiation. So we could conclude that the porous Pd NPs shows higher photothermal stability than that of Au nanorods.

Comparing with other reported photothermal agents, the porous Pd NPs we synthesized possess a few advantages. The size is relatively small (≤ 30 nm), which may increase their blood half-life and reduce removal by the reticuloendothelial system (RES). And the porous Pd NPs exhibit good photothermal stability, while the Au nanorods could melt and lost their NIR absorption under laser irradiation, organic NPs for PTT face serious photobleaching problem[37]. Additionally, the broad absorption nature in NIR region of porous Pd NPs allow us to choose multiple laser wavelengths for PTT application. In this work we demonstrated effective photothermal cancer therapy by using 808 nm and 730 nm laser. Photothermal agents like copper based inorganic nanomaterial performed photothermal ablation of cancer cells by 980 nm laser[14-16], it is reported that the 980 nm laser has the over-heating phenomenon when irradiated at biological tissues because large amount of laser energy may be absorbed by water[38]. In contrast, 808 nm laser is more "cool" than 980 nm laser. Our finding in this study provides a new insight in developing photothermal agents.

Conclusions

In summary, we prepared small Pd NPs with a special porous architecture, which exhibit superior performance in PTT to solid Pd nanocubes due to the enhanced NIR absorption. The photothermal conversion efficiency of porous Pd is as high as

93.4%, comparable to typical gold nanorods. In the presence of porous Pd NPs (with a concentration as low as 23 μg/mL), almost 100% HeLa cells were destructed after 4 min illumination with an 808 nm laser (at power density of 8 W/cm^2), and 70% cells were killed after 4 min irradiation with a 730 nm laser (power density 6 W/cm^2). These results demonstrated the efficacy of our porous Pd NPs for photothermal therapy. As the size of porous Pd NPs is relatively small, it would prolong the blood circulation time when it is administrated to live animal body. And the porous structure of Pd NPs may allow us to deliver drug into cancer cell. We believe this porous Pd structure holds great potential in photothermal therapy and drug delivery.

Acknowlegment

This work was supported by NSFC (Nos. 20971005 and 20931160429) and MOST of China (No.2011AA03A407).

Notes and references

Beijing National Laboratory for Molecular Sciences, State Key Laboratory of Rare Earth Materials Chemistry and Applications, PKU-HKU Joint Laboratory in Rare Earth Materials and Bioinorganic Chemistry, Peking University, Beijing 100871, China. Fax: +86-10-62754179; Tel: +86-10-62754179; Email: sun@pku.edu.cn, yan@pku.edu.cn.

† Electronic Supplementary Information (ESI) available: [The detailed photothermal conversion efficiency calculation, TEM images and extinction spectra of small sized Pd NPs and broad sized Pd polyhedra, TEM image of porous Pd NPs after mPEG-SH modification, additional *in vitro* photothermal therapy results and photothermal stability comparision of porous Pd NPs and Au nanorods under 808 nm laser irradiation can be found in ESI]. See DOI: 10.1039/b000000x/

1 L. C. Kennedy, L. R. Bickford, N. A. Lewinski, A. J. Coughlin, Y. Hu, E. S. Day, J. L. West and R. A. Drezek, *Small*, 2011, **7**, 169-183.

2 R. Weissleder, *Nat. Biotechnol.*, 2001, **19**, 316-317.

3 J. V. Frangioni, *Curr. Opin. Chem. Biol.*, 2003, **7**, 626-634.

4 S. J. Soenen, P. Rivera-Gil, J. M. Montenegro, W. J. Parak, S. C. De Smedt and K. Braeckmans, *Nano Today*, 2011, **6**, 446-465.

5 H. S. Choi, W. Liu, P. Misra, E. Tanaka, J. P. Zimmer, B. I. Ipe, M. G. Bawendi and J. V. Frangioni, *Nat. Biotechnol.*, 2007, **25**, 1165-1170.

6 F. Osaki, T. Kanamori, S. Sando, T. Sera and Y. Aoyama, *J. Am. Chem. Soc.*, 2004, **126,** 6520-6521.

7 B. D. Chithrani, A. A. Ghazani and W. C. W. Chan, *Nano Lett.*, 2006, **6**, 662-668.

8 X. H. Zheng, F. F. Zhou, B. Y. Wu, W. R. Chen and D. Xing, *Mol. Pharmaceutics*, 2012, **9**, 514-522.

9 K. Yang, H. Xu, L. Cheng, C. Y. Sun, J. Wang and Z. Liu, *Adv. Mater.*, 2012, **24**, 5586-5592.

10 H. K. Moon, S. H. Lee and H. C. Choi, *ACS Nano*, 2009, **3**, 3707-3713.

11 K. Yang, S. A. Zhang, G. X. Zhang, X. M. Sun, S. T. Lee and Z. A. Liu, *Nano Lett.*, 2010, **10**, 3318-3323.

12 K. Yang, L. Z. Feng, X. Z. Shi and Z. Liu, *Chem. Soc. Rev.*, 2013, **42**, 530-547.

13 X. Q. Huang, S. H. Tang, X. L. Mu, Y. Dai, G. X. Chen, Z. Y. Zhou, F. X. Ruan, Z. L. Yang and N. F. Zheng, *Nat. Nanotechnol.*, 2011, **6**, 28-32.

14 Q. W. Tian, M. H. Tang, Y. G. Sun, R. J. Zou, Z. G. Chen, M. F. Zhu, S. P. Yang, J. L. Wang, J. H. Wang and J. Q. Hu, *Adv. Mater.*, 2011, **23**, 3542-3547.

15 Q. W. Tian, F. R. Jiang, R. J. Zou, Q. Liu, Z. G. Chen, M. F. Zhu, S. P. Yang, J. L. Wang, J. H. Wang and J. Q. Hu, *ACS Nano*, 2011, **5**, 9761-9771.

16 C. M. Hessel, V. P. Pattani, M. Rasch, M. G. Panthani, B. Koo, J. W. Tunnell and B. A. Korgel, *Nano Lett.*, 2011, **11**, 2560-2566.

17 X. H. Huang, S. Neretina and M. A. El-Sayed, *Adv. Mater.*, 2009, **21**, 4880-4910.

18 X. H. Huang, I. H. El-Sayed, W. Qian and M. A. El-Sayed, *J. Am. Chem. Soc.*, 2006, **128**, 2115-2120.

19 H. C. Huang, K. Rege and J. J. Heys, *ACS Nano*, 2010, **4**, 2892-2900.

20 S. Lal, S. E. Clare and N. J. Halas, *Acc. Chem. Res.*, 2008, **41**, 1842-1851.

21 J. Y. Chen, C. Glaus, R. Laforest, Q. Zhang, M. X. Yang, M. Gidding, M. J. Welch and Y. N. Xia, *Small*, 2010, **6**, 811-817.

22 H. Yuan, A. M. Fales and T. Vo-Dinh, *J. Am. Chem. Soc.*, 2012, **134**, 11358-11361.

23 Y. C. Wang, K. C. L. Black, H. Luehmann, W. Y. Li, Y. Zhang, X. Cai, D. H. Wan, S. Y. Liu, M. Li, P. Kim, Z. Y. Li, L. H. V. Wang, Y. J. Liu and Y. A. Xia, *ACS Nano*, 2013, **7**, 2068-2077.

24 B. Nikoobakht and M. A. El-Sayed, *Chem. Mater.*, 2003, **15**, 1957-1962.

25 L. R. Hirsch, R. J. Stafford, J. A. Bankson, S. R. Sershen, B. Rivera, R. E. Price, J. D. Hazle, N. J. Halas and J. L. West, *P. Natl. Acad. Sci. USA*, 2003, **100**, 13549-13554.

26 M. R. Rasch, K. V. Sokolov and B. A. Korgel, *Langmuir*, 2009, **25**, 11777-11785.

27 S. Link, C. Burda, M. B. Mohamed, B. Nikoobakht and M. A. El-Sayed, *J. Phys. Chem. A*, 1999, **103**, 1165-1170.

28 G. Akchurin, B. Khlebtsov, G. Akchurin, V. Tuchin, V. Zharov and N. Khlebtsov, *Nanotechnology*, 2008, **19**, 015701.

29 S. H. Tang, X. Q. Huang and N. F. Zheng, *Chem. Commun.*, 2011, **47**, 3948-3950.

30 F. Wang, C. H. Li, L. D. Sun, C. H. Xu, J. F. Wang, J. C. Yu and C. H. Yan, *Angew. Chem., Int. Ed.*, 2012, **51**, 4872-4876.

31 F. Wang, L. D. Sun, W. Feng, H. J. Chen, M. H. Yeung, J. F. Wang and C. H. Yan, *Small*, 2010, **6**, 2566-2575.

32 Y. X. Zhao, H. C. Pan, Y. B. Lou, X. F. Qiu, J. J. Zhu and C. Burda, *J. Am. Chem. Soc.*, 2009, **131**, 4253-4261.

33 N. W. S. Kam, M. O'Connell, J. A. Wisdom and H. J. Dai, *P. Natl. Acad. Sci. USA*, 2005, **102**, 11600-11605.

34 B. Nikoobakht, J. P. Wang and M. A. El-Sayed, *Chem. Phys. Lett.*, 2002, **366**, 17-23.

35 H. J. Chen, L. Shao, T. A. Ming, Z. H. Sun, C. M. Zhao, B. C. Yang and J. F. Wang, *Small*, 2010, **6**, 2272-2280.

36 M. P. Melancon, W. Lu, Z. Yang, R. Zhang, Z. Cheng, A. M. Elliot, J. Stafford, T. Olson, J. Z. Zhang and C. Li, *Mol. Cancer Ther.*, 2008, **7**, 1730-1739.

37 J. Yu, D. Javier, M. A. Yaseen, N. Nitin, R. Richards-Kortum, B. Anvari and M. S. Wong, *J. Am. Chem. Soc.*, 2010, **132**, 1929-1938.

38 Y. F. Wang, G. Y. Liu, L. D. Sun, J. W. Xiao, J. C. Zhou and C. H. Yan, *ACS Nano*, 2013, **7**, 7200-7206.

Graphical Abstract

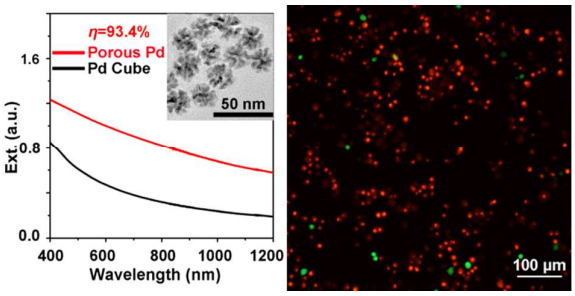

In this article, we report the Pd NPs with specious porous structure exhibit enhanced near infrared (NIR) absorption and enhanced photothermal effect compared with Pd nanocubes with similar size. When dispersed in water and illuminated with an 808 nm laser, the porous Pd NPs give a photothermal conversion efficiency as high as 93.4%. The porous Pd nanostructure shows very high efficacy in photothermal ablation of HeLa cells.